

# Dileptons and Chiral Symmetry Restoration

P. M. Hohler and R. Rapp

*Department of Physics and Astronomy and Cyclotron Institute, Texas A&M University, College Station, TX 77843-3366, USA*

## Abstract

We report on recent work relating the medium effects observed in dilepton spectra in heavy-ion collisions to potential signals of chiral symmetry restoration. The key connection remains the approach to spectral function degeneracy between the vector-isovector channel with its chiral partner, the axialvector-isovector channel. Several approaches are discussed to elaborate this connection, namely QCD and Weinberg sum rules with input for chiral order parameters from lattice QCD, and chiral hadronic theory to directly evaluate the medium effects of the axialvector channel and the pertinent pion decay constant as function of temperature. A pattern emerges where the chiral mass splitting between  $\rho$  and  $a_1$  burns off and is accompanied by a strong broadening of the spectral distributions.

*Keywords:*

## 1. Introduction

The search for signals of chiral symmetry restoration (CSR) in hot/dense QCD matter remains one of the key objectives, and challenges, in relativistic heavy-ion physics. Since the spontaneous breaking of chiral symmetry (SBSC) in the QCD vacuum is an inherently soft phenomenon, occurring at scales of around 1 GeV and below, low-mass dilepton spectra are arguably one of the most promising observables to detect changes in the chiral properties of the finite-temperature/-density ground state. The low-mass dilepton emissivity, which governs thermal radiation from a hot fireball, is directly proportional to the hadronic vector ( $J^P=1^-$ ) spectral function of the system. In vacuum, its low-mass spectral strength is concentrated in the light vector mesons  $\rho$ ,  $\omega$  and  $\phi$ , representing massive hadronic degrees of freedom as manifestations of the nontrivial condensate structure of the QCD vacuum. At the quark level, SBSC is associated with the formation of the quark condensate giving rise to the mass of constituent quarks,  $m_q^* \simeq -G\langle 0|\bar{q}q|0\rangle \simeq 0.3\text{--}0.4\text{ GeV}$ , which in turn form the building blocks of the hadrons. At the hadronic level, SBSC emerges as the splitting of chiral multiplets, such as  $\pi$ - $\sigma$ ,  $N$ - $N^*(1535)$  or  $\rho$ - $a_1$ . Thus, to extract signatures

of (the approach to) CSR from dilepton spectra, which are dominated by the  $\rho$  channel, one is led into investigations of medium effects in the  $a_1$  channel.

The case for investigations of hadronic mechanisms for chiral restoration in the context of dileptons is further motivated by the following considerations. From the phenomenological side, it is rather well established by now that the low-mass enhancement observed in all experiments, ranging from SIS ( $\sqrt{s}=2.25\text{ GeV}$ ) [3] via SPS ( $\sqrt{s}=8.8, 17.3\text{ AGeV}$ ) [4, 5, 6] via the RHIC beam energy scan to its maximal energy ( $\sqrt{s}=19.6, 27, 39, 62, 200\text{ AGeV}$ ) [7, 8], can be understood via thermal radiation of predominantly hadronic origin with a strongly broadened  $\rho$  spectral function, cf. Fig. 1. From the theoretical side, one can estimate the energy density corresponding to hot matter at the pseudo-critical temperature for chiral restoration,  $T_{pc} \simeq 155\text{ MeV}$  (at vanishing baryon chemical potential,  $\mu_B=0$ ). One finds  $\epsilon_{pc} \simeq 0.3\text{ GeV}$  which is comparable to that of cold nuclear matter at twice saturation density. Of course, one should keep in mind that the chiral condensate at  $T_{pc}$  is still at about half of its vacuum value, which, again is in the vicinity of recent estimates in cold nuclear matter at twice nuclear saturation density [13].

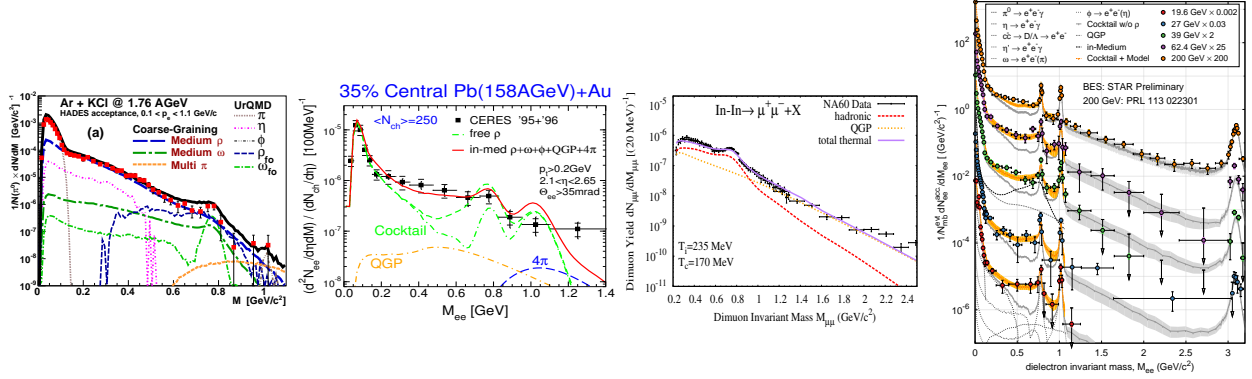


Figure 1: Dilepton spectra in heavy-ion collisions from HADES at SIS [3] (left), CERES [5] and NA60 [6] at SPS (middle panels) and STAR [7] at RHIC (right panel), compared to theoretical calculations with QGP and hadronic emission using the same model for the in-medium  $\rho$  spectral function [9, 10, 11, 12].

In the following, we will present two frameworks of assessing the in-medium changes of the chiral properties of the QCD medium in terms of the vector-axialvector spectral functions. In the first one (Sec. 2), we utilize chiral and QCD sum rules to search for solutions for the axialvector spectral function given previously calculated in-medium  $\rho$  spectral functions and chiral order parameters as available from lattice-QCD as input. In the second one (Sec. 3), we compute vector and axialvector spectral functions in a hot pion gas from a chiral effective theory and extract the in-medium dependence of the pion decay constant and scalar condensate. We conclude in Sec. 4.

## 2. QCD and Weinberg Sum Rules

The QCD sum rule (QCDSR) technique has been widely used to analyze hadronic properties in both vacuum and medium, by relating the pertinent spectral function to an expansion in Euclidean momentum transfer where coefficients are given by vacuum condensates [14]. For the vector channel in vacuum, after a Borel transform to improve convergence, it takes the form

$$\frac{1}{M^2} \int_0^\infty ds \frac{\rho_V(s)}{s} e^{-s/M^2} = \frac{1}{8\pi^2} \left( 1 + \frac{\alpha_s}{\pi} \right) + \frac{m_q \langle \bar{q}q \rangle}{M^4} + \frac{1}{24M^4} \langle \frac{\alpha_s}{\pi} G_{\mu\nu}^2 \rangle - \frac{\pi\alpha_s}{M^6} \frac{56}{81} \langle O_4^V \rangle, \quad (1)$$

and similarly for the axialvector channel with sign changes (and slightly different coefficients) for the chiral odd contributions from the 2- and 4-quark condensates (additional higher twist contributions arise in a heat bath). As is well known for the  $\rho$  meson [15, 16, 17], the QCDSR cannot uniquely predict the in-medium

properties of the spectral function, but it can provide constraints on model calculations.

Weinberg sum rules (WSRs) relate chiral order parameters to energy moments of the difference between the vector and axialvector spectral functions [18],

$$f_n = \int_0^\infty \frac{ds}{\pi} s^n [\rho_V(s) - \rho_A(s)] \quad (2)$$

with  $f_{-1} = f_\pi^2$ ,  $f_0 = f_\pi^2 m_\pi^2 = -2m_q \langle \bar{q}q \rangle$ , and  $f_1 = -2\pi\alpha_s O_4^{\text{SB}}$  (the latter is the chirally odd combination of  $O_4^{V,A}$ ). They have been extended to finite temperature in Ref. [19].

In Ref. [20], our idea was to combine the constraining power of QCDSRs and WSRs to test whether the in-medium  $\rho$  spectral function that underlies the description of dilepton spectra in Fig. 1 is compatible with chiral restoration (see also Ref. [21]). As additional input to the sum rules the temperature dependence for  $f_\pi(T)$  and  $\langle \bar{q}q \rangle(T)$  was taken from lattice QCD data for the latter, and inferred via the Gellmann-Oakes Renner relation for the former. The  $T$  dependence of the 4-quark condensates is less straightforward. We employed current algebra for the contributions from the Goldstone bosons and the standard factorization assumption (valid in a large- $N_c$  expansion) for all other hadrons, augmented with a  $T^{10}$  correction term to render the  $O_4$ 's vanishing at the same temperature as the  $\langle \bar{q}q \rangle$  condensate. The question was then whether an in-medium axialvector spectral function could be found to satisfy the 2 QCDSRs and 3 WSRs. As a starting point, we employed a previously constructed quantitative description of the axial-/vector spectral functions in vacuum as measured in hadronic  $\tau$  decays, which, in addition to the  $\rho$  and  $a_1$ , include one excited state in each channel ( $\rho'$  and  $a_1'$ ) and a chirally invariant (degenerate) continuum [22].

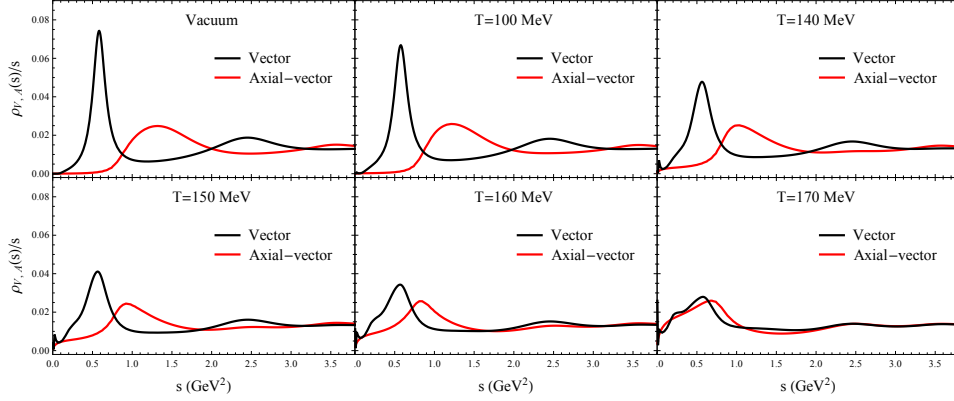


Figure 2: Finite-temperature vector (black curve) and axialvector (red curve) spectral functions from sum rule analysis [20].

First, we tested the the QCDSR for the vector channel. It turned out that this was satisfied well within the typical 1% benchmark, including a small correction to the vector dominance coupling constant being reduced by around 5%. To facilitate the search for an in-medium axialvector spectral function, we augmented the vacuum fit by a 4-parameter ansatz for the in-medium changes of mass, width (2), and coupling strength, and treated the  $T$  dependence of the excited states via chiral mixing. We then searched for minima in the quadratic sum of the deviations of the axialvector QCDSR and the first and second WSR ( $n=-1$  and 0 in Eq. (2); the 3. WSR is beset with larger uncertainty already in vacuum but still satisfied in medium at a comparable level). A smoothly varying in-medium axialvector spectral function could be found which varies smoothly with temperature and satisfies the SRs at the same level of accuracy as in vacuum. The result is compared to the vector spectral function in Fig. 2, showing their progression toward degeneracy. This study shows that the  $\rho$  spectral function underlying the description of dilepton spectra is compatible with the dropping quark condensate computed in lattice QCD and suggests that chiral restoration is satisfied by a combined broadening and burning-off of the  $\rho$ - $a_1$  mass splitting.

### 3. Massive-Yang Mills Chiral Lagrangian

The local-gauge procedure was the method of choice to introduce axial-/vector mesons into chiral pion Lagrangians for many years, via Massive Yang-Mills [23] or Hidden Local Symmetry [24, 25] approaches. However, it turned out to be rather challenging to quantitatively describe the vacuum axial-/vector spectral func-

tions in these approaches, as the single gauge coupling constant does not seem to generate enough strength in the axialvector channel. In Ref. [26], we found that the implementation of a resummed (broad)  $\rho$  spectral function into the vacuum  $a_1$  selfenergy, along with (rather involved) vertex corrections required to maintain chiral symmetry, can largely overcome this problem and yield fair description of the vacuum data.

The next step is to implement this approach at finite temperature, which we have carried out in recent work for a pion gas [27]. The vector and axialvector selfenergies have been evaluated within the Matsubara formalism accounting for medium effects through unitarity cuts (Bose enhancement in decay diagrams such as  $\rho \rightarrow \pi\pi$  and  $a_1 \rightarrow \pi\rho$ ), Landau cuts (scattering diagrams with an incoming thermal pion such as  $\pi\rho \rightarrow a_1$  or  $\pi a_1 \rightarrow \rho$ ), vertex corrections and tadpole diagrams. We have verified that the model-independent low-temperature chiral properties (*e.g.*, no axial/vector meson mass shifts at order  $O(T^2)$  in the chiral limit) are satisfied within our approach. The resulting temperature progression of the vector and axialvector spectral functions is shown in Fig. 3. The  $\rho$  resonance only undergoes a moderate broadening of up to  $\sim 50$  MeV at  $T=160$  MeV, which is in line with previous pion gas studies for Bose enhancement and  $\pi\rho \rightarrow a_1$  resonance excitations. The  $a_1$  resonance exhibits stronger modifications, by developing a larger in-medium width, a reduction in its mass and a low-mass excitation caused by the  $\pi a_1 \rightarrow \rho$  excitation (“chiral mixing”). These features are qualitatively similar to what we found within the sum rule analysis discussed in the previous section. They are also rather robust between employing a linear or non-linear realization of chiral symmetry in the pion

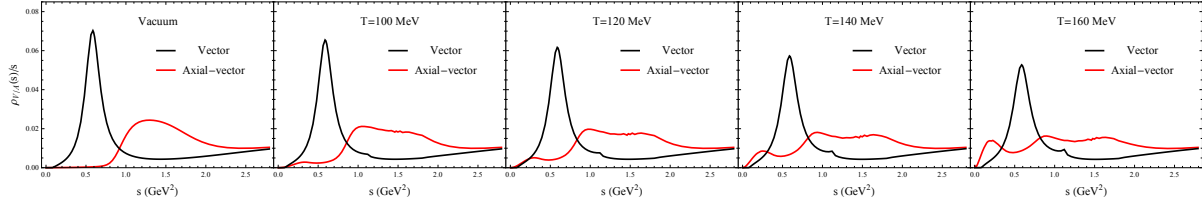


Figure 3: Finite- $T$  vector and axialvector spectral functions within the non-linear realization of Massive Yang-Mills [27].

Lagrangian (the former involves an additional  $\sigma$  field).

The main benefit of a microscopic chiral approach is that one can utilize it to calculate chiral order parameters. We have evaluated both the pion decay constant,  $f_\pi(T)$ , and, within the linear realization, the scalar condensate,  $\sigma(T)$ , and found that both quantities drop by up to 15-20% at  $T=160$  MeV. This corroborates that the trend toward degeneracy in the spectral functions is indeed coupled to an approach toward chiral restoration.

#### 4. Conclusions

We have analyzed the in-medium properties of  $\rho$  and  $a_1$  in the context of the approach toward chiral restoration. First, evaluating QCD and Weinberg sum rules with a realistic in-medium  $\rho$  spectral function and condensates taken from lattice QCD, we found a solution for the axialvector spectral function which smoothly degenerates with the  $\rho$  via a combined broadening and burning-off of the chiral mass splitting. We then utilized a Massive-Yang Mills approach for  $\rho$  and  $a_1$  mesons with realistic vacuum spectral functions to evaluate medium effects in a hot pion gas. Also here, a spectral broadening was accompanied by a reduction in the  $a_1$  mass. This trend toward spectral degeneracy is coupled to a reduction in the pion decay constant evaluated within the same approach. While baryons are not yet included in this calculation, it is interesting to note that a recent study of the correlation functions of the nucleon and its chiral partner,  $N^*(1535)$ , at finite temperature found the latter's mass to drop toward, and ultimately degenerate with, the nucleon mass [28]. This is quite in line with our findings for the vector-axialvector channels, and suggests a general hadronic mechanism of chiral restoration, where the mass splitting in chiral multiplets burns off while the ground-state masses are rather stable with temperature. Indeed, the latter feature is quantitatively consistent with the observed spectral shape of thermal dilepton radiation in heavy-ion collisions, recall Fig. 1.

**Acknowledgments.** This work has been supported by the US-NSF under grant No. PHY-1306359.

#### References

- [1] S. Borsanyi *et al.*, JHEP **1009** (2010) 073.
- [2] T. Bhattacharya *et al.*, Phys. Rev. Lett. **113** (2014) 082001.
- [3] G. Agakichiev *et al.* [HADES Collaboration], Phys. Rev. C **84** (2011) 014902.
- [4] D. Adamova *et al.* [CERES/NA45 Collaboration], Phys. Rev. Lett. **91** (2003) 042301.
- [5] G. Agakichiev *et al.* [CERES Collaboration], Eur. Phys. J. C **41** (2005) 475.
- [6] H.J. Specht [NA60 Collaboration], AIP Conf. Proc. **1322** (2010) 1.
- [7] P. Huck [STAR Collaboration], Nucl. Phys. A **931** (2014) 659.
- [8] L. Adamczyk *et al.* [STAR Collaboration], Phys. Rev. C **92** (2015) 024912.
- [9] S. Endres, H. van Hees, J. Weil and M. Bleicher, Phys. Rev. C **92** (2015) 1, 014911.
- [10] H. van Hees and R. Rapp, Nucl. Phys. A **806** (2008) 339.
- [11] R. Rapp and H. van Hees, arXiv:1411.4612 [hep-ph].
- [12] R. Rapp, Adv. High Energy Phys. **2013** (2013) 148253.
- [13] J.W. Holt, N. Kaiser and W. Weise, Prog. Part. Nucl. Phys. **73** (2013) 35.
- [14] M.A. Shifman, A.I. Vainshtein and V.I. Zakharov, Nucl. Phys. B **147** (1979) 385; 448.
- [15] T. Hatsuda, Y. Koike and S.-H. Lee, Nucl. Phys. B **394** (1993) 221.
- [16] S. Leupold, W. Peters and U. Mosel, Nucl. Phys. A **628** (1998) 311.
- [17] S. Zschocke, O.P. Pavlenko and B. Kämpfer, Eur. Phys. J. A **15** (2002) 529.
- [18] S. Weinberg, Phys. Rev. Lett. **18** (1967) 507.
- [19] J.I. Kapusta and E.V. Shuryak, Phys. Rev. D **49** (1994) 4694.
- [20] P.M. Hohler and R. Rapp, Phys. Lett. B **731** (2014) 103.
- [21] A. Ayala, C.A. Dominguez, M. Loewe and Y. Zhang, Phys. Rev. D **90** (2014) 034012.
- [22] P.M. Hohler and R. Rapp, Nucl. Phys. A **892** (2012) 58.
- [23] H. Gomm, O. Kaymakcalan and J. Schechter, Phys. Rev. D **30** (1984) 2345.
- [24] M. Bando, T. Kugo and K. Yamawaki, Phys. Rept. **164** (1988) 217.
- [25] M. Harada and K. Yamawaki, Phys. Rept. **381** (2003) 1.
- [26] P.M. Hohler and R. Rapp, Phys. Rev. D **89** (2014) 125013.
- [27] P.M. Hohler and R. Rapp, in preparation.
- [28] G. Aarts, C. Allton, S. Hands, B. Jaeger, C. Praki and J. I. Skullerud, Phys. Rev. D **92** (2015) 014503.